

## Phosphonate-Based Bipyridine Dyes for Stable Photovoltaic Devices

Isabelle Gillaizeau-Gauthier,<sup>†</sup> Fabrice Odobel,<sup>\*,†</sup>  
 Monica Alebbi,<sup>‡</sup> Roberto Argazzi,<sup>‡</sup> Emiliana Costa,<sup>‡</sup>  
 Carlo Alberto Bignozzi,<sup>\*,‡</sup> Ping Qu,<sup>§</sup> and  
 Gerald J. Meyer<sup>\*,§</sup>

Laboratoire de Synthèse Organique, UMR 6513 CNRS,  
 Faculté des Sciences et des Techniques de Nantes, BP  
 92208, 2, rue de la Houssinière, 44322 Nantes Cedex 03,  
 France, Dipartimento di Chimica dell'Università di Ferrara,  
 Via L. Borsari 46, 44100 Ferrara, Italy, and Department of  
 Chemistry, Johns Hopkins University, 3400 North Charles  
 Street, Baltimore, Maryland 21218

Received February 15, 2001

### Introduction

The dye sensitization of nanocrystalline TiO<sub>2</sub> electrodes has been intensely investigated for solar energy conversion.<sup>1</sup> In dye-sensitized solar cells, the dye molecules “sensitize” the semiconductor to visible radiation that would otherwise be transmitted. The dye molecules are therefore generically referred to a “sensitizers”. The most successful sensitizers for applications in regenerative solar cells are ruthenium polypyridyl compounds anchored to nanocrystalline TiO<sub>2</sub> surfaces via carboxylic acid groups.<sup>1,2</sup> However, other kinds of chemical bonds, based on silanes,<sup>3</sup> amides,<sup>4</sup> ethers,<sup>5</sup> acetylacetonates,<sup>6</sup> and phosphonates,<sup>7</sup> have also been used to attach photoactive and redox-active molecules to metal oxide surfaces.<sup>3–7</sup> The highly oxophilic phosphonic acid group has been reported to provide a strong chemical attachment, most probably because of its affinity to hard acid metals such as Ti(IV) in TiO<sub>2</sub>.<sup>8</sup>

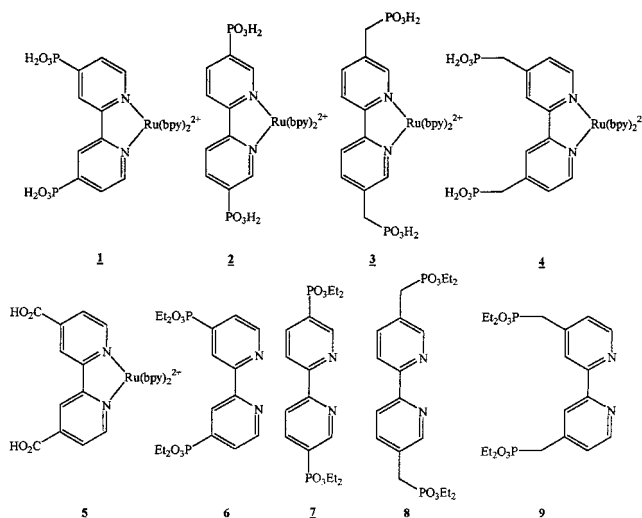
<sup>†</sup> Faculté des Sciences et des Techniques de Nantes.

<sup>‡</sup> Università di Ferrara.

<sup>§</sup> Johns Hopkins University.

- (1) O'Regan, B.; Grätzel, M. *Nature* **1991**, *353*, 737–739. (b) Nazeeruddin, M. K.; Kay, A.; Rodicio, I.; Humphry-Baker, R.; Müller, E.; Liska, P.; Vlachopoulos, N.; Grätzel, M. *J. Am. Chem. Soc.* **1993**, *115*, 6382–6390.
- (2) Argazzi, R.; Bignozzi, C. A.; Heimer, T. A.; Castellano, F. N.; Meyer, G. J. *Inorg. Chem.* **1994**, *33*, 5741–5749.
- (3) (a) Ghosh, P.; Spiro, T. G. *J. Am. Chem. Soc.* **1980**, *102*, 5543–5549. (b) Bookbinder, D. C.; Wrighton, M. S. *J. Electrochem. Soc.* **1983**, *130*, 1080–1086. (c) Miller, C. J.; Widrig, C. A.; Charych, D. H.; Majda, M. J. *J. Phys. Chem.* **1988**, *92*, 1928–1933. (d) Ford, W. E.; Rodgers, M. A. *J. Phys. Chem.* **1994**, *98*, 3822–3841.
- (4) (a) Moses, P. R.; Murray, R. W. *J. Electroanal. Chem.* **1977**, *77*, 393–400. (b) Shepard, V. R.; Armstrong, N. R. *J. Phys. Chem.* **1979**, *83*, 1268–1276. (c) Fox, M. A.; Nabs, F. J.; Voynick, T. A. *J. Am. Chem. Soc.* **1980**, *102*, 4036–4042.
- (5) Zou, C.; Wrighton, M. S. *J. Am. Chem. Soc.* **1990**, *112*, 7578–7586.
- (6) Heimer, T. A.; D'Arangelis, S. T.; Farzard, F.; Stipkala, J. M.; Meyer, G. J. *Inorg. Chem.* **1996**, *35*, 5319–5324.
- (7) (a) Péchy, P.; Rotzinger, F. P.; Nazeeruddin, M. K.; Kohle, O.; Zakeeruddin, S. M.; Humphry-Baker, R.; Grätzel, M. *Chem. Commun.* **1995**, 65–66. (b) Yan, S. G.; Hupp, J. T. *J. Phys. Chem.* **1996**, *100*, 6867–6870. (c) Saube, G. B.; Mallouk, T. E.; Kim, W.; Schmehl, R. H. *J. Phys. Chem. B* **1997**, *101*, 2508–2513. (d) Zakeeruddin, S. M.; Nazeeruddin, M. K.; Péchy, P.; Rotzinger, F. P.; Humphry-Baker, R.; Kalyanasundaram, K.; Grätzel, M. *Inorg. Chem.* **1997**, *36*, 5937–5946. (e) Jing, B.; Zhang, H.; Lu, Z.; Shen, T. *J. Mater. Chem.* **1998**, *8*, 2055–2060. (f) Zaban, A.; Ferrere, S.; Gregg, B. A. *J. Phys. Chem. B* **1998**, *102*, 542. (g) Trammell, S.; Moss, J. A.; Yang, J.; Slate, B. M.; Nakhle, M.; Slate, C. A.; Odobel, F.; Sykora, M.; Erickson, B. W.; Meyer, T. J. *Inorg. Chem.* **1999**, *38*, 3665–3669.

### Chart 1. Complexes and Ligands Used in This Work



In this paper, we report the synthesis, photophysical properties, surface attachment, and photoelectrochemical properties of a series of ruthenium(II) bipyridyl complexes with phosphonic acid functional groups (Chart 1). All the Ru<sup>II</sup> complexes are composed of a Ru(bpy)<sub>2</sub><sup>2+</sup> core and differ only in the one bipyridine ligand substituted with phosphonic acid functional groups for surface attachment. The compounds synthesized allow two important comparisons to be made. The first is between sensitizers that differ only in the position of the phosphonic acid groups for surface attachment, i.e., 4,4' vs 5,5'. The second comparison is between sensitizers substituted in the same position but with or without an intervening methylene spacer between the bipyridine ligand and phosphonic acid group, i.e., –CH<sub>2</sub>PO<sub>3</sub>H<sub>2</sub> vs –PO<sub>3</sub>H<sub>2</sub>. The results of this study demonstrate that, through rational sensitizer design, it is possible to achieve efficient sensitization of semiconductors by complexes with a saturated methylene spacer between the anchoring group and the chromophoric bipyridine ligand.

### Experimental Section

**Materials.** Solvents and materials were purchased from Aldrich-Fluka and used without further purification. RuCl<sub>3</sub>·3H<sub>2</sub>O was bought from Johnson Matthey-Alfa, and Sephadex LH20 was purchased from Pharmacia. The resin was allowed to swell in the appropriate solvent for a minimum of 2 h before use. 4,4'-Dicarboxy-2,2'-bipyridine and *cis*-[Ru(bpy)<sub>2</sub>Cl<sub>2</sub>]<sub>2</sub>·2H<sub>2</sub>O were prepared and purified as described in the literature.<sup>9,10</sup> The compound Ru(4,4'-(CO<sub>2</sub>H)<sub>2</sub>bpy)<sub>2</sub>(NCS)<sub>2</sub> was available from previous studies.<sup>2</sup>

**Measurements.** <sup>1</sup>H NMR spectra were recorded on a Varian Gemini 300 at 25 °C and on a Bruker AMX 400 at 25 °C. Chemical shifts are reported relative to the solvent reference. For D<sub>2</sub>O, TMS was used as an internal standard. The peak assignments are given as follows: chemical shifts in ppm (the number of protons involved and the multiplicity of the signal are in parentheses): s, singlet; d, doublet; t, triplet; m, multiplet. In ruthenium complexes, ancillary bipyridine protons are labeled as H<sub>a</sub>, whereas phosphonated bipyridine has only the proton position attachment as a subscript. <sup>31</sup>P{<sup>1</sup>H} NMR spectra

(8) Trummell, S.; Wimbish, J.; Meyer, T. J.; Odobel, F. *J. Am. Chem. Soc.* **1998**, *120*, 13248–13249.

(9) Oki, A. R.; Morgan, R. J. *Synth. Commun.* **1995**, 25.

(10) Sullivan, B. P.; Salmon, D. J.; Meyer, T. J. *Inorg. Chem.* **1978**, *17*, 3334.

were measured at 25 °C using a Bruker AC-200 spectrometer; chemical shifts in ppm were referenced to external 85% H<sub>3</sub>PO<sub>4</sub>.

FAB-MS analyses were performed in a *m*-nitrobenzyl alcohol matrix (MBA) on a ZAB-HF-FAB (fast atom bombardment) spectrometer.

Spectroscopic, electrochemical, and photoelectrochemical measurements and TiO<sub>2</sub> film preparations were carried out following previously reported procedures.<sup>11</sup>

Transient absorption data were acquired as previously described.<sup>12</sup> The electron injection quantum yields ( $\phi$ ) were determined by comparative actinometry, using tris(2,2'-bipyridyl)ruthenium(II) chloride in a poly(methyl methacrylate) (PMMA) thin film deposited on a microscope slide as a reference actinometer,  $\Delta\epsilon_{450} = (-1.0 \pm 0.09) \times 10^4 \text{ M}^{-1} \text{ cm}^{-1}$ , as previously described.<sup>12</sup> The ground state–excited state isosbestic points of the complexes were determined through transient absorption measurement on ZrO<sub>2</sub>. The  $\Delta\epsilon$  at the ground state–excited state isosbestic point was determined by spectroelectrochemistry of the TiO<sub>2</sub>-bound sensitizers. The ground state absorbance of the actinometer and the sensitized colloidal films were approximately absorbance matched at the excitation wavelength. Quantum yield calculations were corrected for any differences in light absorbed by the actinometer and the thin film samples.

#### General Procedure for the Preparation of Ruthenium Complexes.

A solution of the phosphonate bipyridine (**6**,<sup>13</sup> **7**,<sup>13</sup> or **8**<sup>14</sup>) (0.5 mmol) and 310 mg (0.6 mmol) of *cis*-[Ru(bpy)<sub>2</sub>Cl<sub>2</sub>] $\cdot$ 2H<sub>2</sub>O<sup>10</sup> in a 50 mL mixture of EtOH/H<sub>2</sub>O (9:1 v:v) was heated at reflux in the dark under an argon atmosphere for 3 h. The solvents were removed by rotary evaporation, and the crude dark red residue was dissolved in a minimum amount of an acetone/water (9:1 v:v) mixture and loaded on a silica gel column. Elution with an acetone/water mixture (8:2 v:v) removed the unreacted Ru(bpy)<sub>2</sub>Cl<sub>2</sub>. More rinsing with an acetone/water/KNO<sub>3</sub> saturated aqueous solution (10 drops of KNO<sub>3</sub> added to a mixture of 80 mL of acetone and 20 mL of water) afforded the desired ester complex with NO<sub>3</sub><sup>-</sup> as counteranion. The pure fractions of the target product were collected and acetone was removed under vacuum. After extraction of the resulting aqueous solution with dichloromethane twice, 0.3 g of KPF<sub>6</sub> was added to precipitate the final product. The organic phase was dried over MgSO<sub>4</sub> and the solvent removed to give the bipyridine ester complex with PF<sub>6</sub><sup>-</sup> anions.

**[Ru(bpy)<sub>2</sub>(4,4'-(PO<sub>3</sub>Et)<sub>2</sub>bpy)](PF<sub>6</sub>)<sub>2</sub>.** Starting from **6**<sup>13</sup> and using the described general procedure, the desired complex was isolated as a red solid with a yield of 70%.

<sup>1</sup>H NMR (400 MHz, CD<sub>3</sub>CN): 1.32 (12H, m) CH<sub>3</sub>; 4.20 (8H, m) CH<sub>2</sub>; 7.45 (4H, m) H<sub>5a</sub>, H<sub>5'a</sub>; 7.64 (2H, m) H<sub>5</sub>, H<sub>5'</sub>; 7.72 (4H, t, *J* = 5 Hz) H<sub>6a</sub>, H<sub>6'a</sub>; 7.95 (2H, dd, *J* = 4 and 6 Hz) H<sub>6</sub>, H<sub>6'</sub>; 8.10 (4H, dt, *J* = 1 and 8 Hz) H<sub>4a</sub>, H<sub>4'a</sub>; 8.54 (4H, d, *J* = 8 Hz) H<sub>3a</sub>, H<sub>3'a</sub>; 8.80 (2H, d, *J* = 13 Hz) H<sub>3</sub>, H<sub>3'</sub>.

<sup>31</sup>P NMR (81 MHz, CD<sub>3</sub>CN,  $\delta$ ): 10.32.

FAB-MS: C<sub>38</sub>H<sub>42</sub>N<sub>6</sub>RuP<sub>2</sub> requires 842, exptl 842.

**[Ru(bpy)<sub>2</sub>(5,5'-(PO<sub>3</sub>Et)<sub>2</sub>bpy)](PF<sub>6</sub>)<sub>2</sub>.** Starting from **7**<sup>13</sup> and using the described general procedure, the ruthenium complex was isolated in 72% yield as a red solid.

<sup>1</sup>H NMR (400 MHz, CD<sub>3</sub>CN): 1.18 (12H, m) CH<sub>3</sub>; 3.98 (8H, m) CH<sub>2</sub>; 7.45 (4H, m) H<sub>5a</sub>, H<sub>5'a</sub>; 7.80 (4H, m) H<sub>6a</sub>, H<sub>6'a</sub>; 7.85 (2H, m) H<sub>6</sub>, H<sub>6'</sub>; 8.12 (4H, m) H<sub>4a</sub>, H<sub>4'a</sub>; 8.34 (2H, m) H<sub>4</sub>, H<sub>4'</sub>; 8.60 (4H, m) H<sub>3a</sub>, H<sub>3'a</sub>; 8.78 (2H, m) H<sub>3</sub>, H<sub>3'</sub>.

<sup>31</sup>P NMR (81 MHz, CD<sub>3</sub>CN,  $\delta$ ): 10.86.

FAB-MS: C<sub>38</sub>H<sub>42</sub>N<sub>6</sub>RuP<sub>2</sub> requires 842, exptl 842.

**[Ru(bpy)<sub>2</sub>(5,5'-(CH<sub>2</sub>PO<sub>3</sub>Et)<sub>2</sub>bpy)]Cl<sub>2</sub>.** Starting from **8**<sup>14</sup> and using the described general procedure, the ruthenium complex was isolated in 82% yield as a red solid.

<sup>1</sup>H NMR (300 MHz, CD<sub>3</sub>CN,  $\delta$ ): 1.05 (12H, m, CH<sub>3</sub>); 3.12 (4H, d, *J* = 21 Hz, CH<sub>2</sub>P); 3.83 (8H, m, CH<sub>2</sub>); 7.42 (4H, m) H<sub>5a</sub>, H<sub>5'a</sub>; 7.67 (2H, m) H<sub>6</sub>, H<sub>6'</sub>; 7.74 (4H, m), H<sub>6a</sub>, H<sub>6'a</sub>; 7.99 (2H, m) H<sub>4</sub>, H<sub>4'</sub>; 8.11 (4H, m) H<sub>4a</sub>, H<sub>4'a</sub>; 8.48 (2H, m) H<sub>3</sub>, H<sub>3'</sub>; 8.58 (4H, m) H<sub>3a</sub>, H<sub>3'a</sub>.

<sup>31</sup>P NMR (81 MHz, D<sub>2</sub>O,  $\delta$ ): 24.21.

FAB-MS: C<sub>40</sub>H<sub>46</sub>F<sub>6</sub>N<sub>6</sub>RuO<sub>6</sub>P<sub>3</sub> requires 1014, exptl 1014.

**General Procedures for the Hydrolysis of the Phosphonate Functional Groups. Method A.** To a solution of the ester bipyridine complex (0.35 mmol) in 20 mL of dry DMF was added 0.6 mL (4.5 mmol) of TMSBr. The mixture was heated at 60 °C under argon in the dark for 18 h. The excess DMF and TMSBr were then removed by heating under vacuum using a liquid nitrogen filled trap. The solid residue was dissolved in MeOH and stirred at room temperature for 3 h in order to hydrolyze the silyl ester. To this deep orange solution was added diethyl ether until precipitation occurred. The red solid was filtered and washed with diethyl ether. Drying under vacuum gave the desired complex.

**Method B.** The ester bipyridine complex (1.3 mmol) was dissolved in 30 mL of 48% HBr and heated at 110 °C in the dark for 12 h. The HBr was then removed under vacuum using a liquid nitrogen filled trap. The solid residue was suspended in MeOH and stirred at room temperature until its total solubilization. After precipitation with ether, filtration, and drying under vacuum the red solid was isolated in 90–95% yield.

**[Ru(bpy)<sub>2</sub>(4,4'-(PO<sub>3</sub>H)<sub>2</sub>bpy)]Br<sub>2</sub> (1).** According to method A, the desired complex **1** was obtained as a red solid in 93% yield.

<sup>1</sup>H NMR (400 MHz, CD<sub>3</sub>OD,  $\delta$ ): 7.51 (4H, m) H<sub>5a</sub>, H<sub>5'a</sub>; 7.75 (2H, m) H<sub>5</sub>, H<sub>5'</sub>; 7.82 (4H, m) H<sub>6a</sub>, H<sub>6'a</sub>; 8.01 (2H, m) H<sub>6</sub>, H<sub>6'</sub>; 8.15 (4H, t, *J* = 8 Hz) H<sub>4a</sub>, H<sub>4'a</sub>; 8.73 (4H, d, *J* = 8 Hz) H<sub>3a</sub>, H<sub>3'a</sub>; 8.91 (2H, d, *J* = 13 Hz) H<sub>3</sub>, H<sub>3'</sub>.

<sup>31</sup>P NMR (81 MHz, CD<sub>3</sub>OD,  $\delta$ ): 6.06.

**[Ru(bpy)<sub>2</sub>(5,5'-(PO<sub>3</sub>H)<sub>2</sub>bpy)]Br<sub>2</sub> (2).** According to method A, the desired complex **2** was obtained as a red solid in 90% yield.

<sup>1</sup>H NMR (400 MHz, D<sub>2</sub>O,  $\delta$ ): 7.37 (4H, m) H<sub>5a</sub>, H<sub>5'a</sub>; 7.81 (4H, m) H<sub>6a</sub>, H<sub>6'a</sub>; 8.00 (2H, m) H<sub>6</sub>, H<sub>6'</sub>; 8.03 (4H, m) H<sub>4a</sub>, H<sub>4'a</sub>; 8.23 (2H, m) H<sub>4</sub>, H<sub>4'</sub>; 8.52 (4H, m) H<sub>3a</sub>, H<sub>3'a</sub>; 8.59 (2H, m) H<sub>3</sub>, H<sub>3'</sub>.

<sup>31</sup>P NMR (81 MHz, D<sub>2</sub>O,  $\delta$ ): 5.91.

**[Ru(bpy)<sub>2</sub>(5,5'-(CH<sub>2</sub>PO<sub>3</sub>H)<sub>2</sub>bpy)]Br<sub>2</sub> (3).** According to method B, complex **3** was isolated as a red solid in 96% yield.

<sup>1</sup>H NMR (200 MHz, D<sub>2</sub>O,  $\delta$ ): 3.12 (4H, d, *J* = 21 Hz, CH<sub>2</sub>P); 7.42 (4H, m) H<sub>5a</sub>, H<sub>5'a</sub>; 7.69 (2H, m) H<sub>6</sub>, H<sub>6'</sub>; 7.88 (4H, m) H<sub>6a</sub>, H<sub>6'a</sub>; 8.00 (2H, m) H<sub>4</sub>, H<sub>4'</sub>; 8.09 (4H, m) H<sub>4a</sub>, H<sub>4'a</sub>; 8.50 (2H, *J* = 8 Hz) H<sub>3</sub>, H<sub>3'</sub>; 8.59 (4H, d, *J* = 8 Hz) H<sub>3a</sub>, H<sub>3'a</sub>.

FAB-MS: C<sub>32</sub>H<sub>30</sub>N<sub>6</sub>RuO<sub>6</sub>P<sub>2</sub> requires 757, exptl 757.

<sup>31</sup>P NMR (81 MHz, D<sub>2</sub>O,  $\delta$ ): 20.89.

**4,4'-Diethoxycarbonyl-2,2'-bipyridine (12).** To a suspension of 4,4'-dicarboxy-2,2'-bipyridine **11**<sup>9</sup> (5.0 g, 20.5 mmol) in 400 mL of absolute ethanol was added 5 mL of concentrated sulfuric acid. The mixture was refluxed for 80 h to obtain a clear solution and then cooled to room temperature. Water (400 mL) was added and the excess ethanol removed under vacuum. The pH was adjusted to neutral with NaOH solution, and the resulting precipitate was filtered and washed with water (pH = 7). The solid was dried to obtain 5.5 g (90%) of **12**.

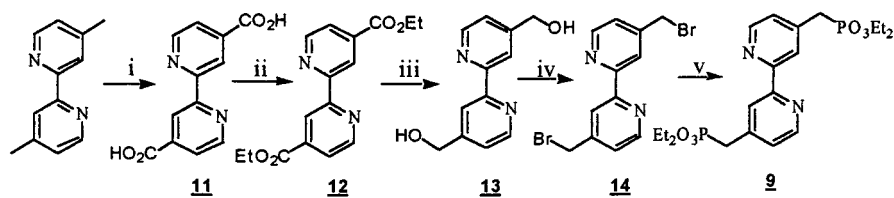
<sup>1</sup>H NMR (300 MHz, CDCl<sub>3</sub>,  $\delta$ ): 1.45 (6H, t, *J* = 7 Hz, CH<sub>3</sub>); 4.48 (4H, q, *J* = 7 Hz, CH<sub>2</sub>); 7.98 (2H, d, *J* = 6 Hz, aryl H on C<sub>5</sub> and C<sub>5'</sub>); 8.88 (2H, d, *J* = 6 Hz, aryl H on C<sub>6</sub> and C<sub>6'</sub>); 9.00 (2H, s, aryl H on C<sub>3</sub> and C<sub>3'</sub>).

Elemental anal. Calcd for C<sub>16</sub>H<sub>16</sub>N<sub>2</sub>O<sub>4</sub>: C, 63.98; H, 5.37; N, 9.33. Found: C, 63.43; H, 5.71; N, 9.57.

**4,4'-Bis(hydroxymethyl)-2,2'-bipyridine (13).** An 8.2 g amount of sodium borohydride was added in one portion to a suspension of the diester **12** (3.0 g, 10.0 mmol) in 200 mL of absolute ethanol. The mixture was refluxed for 3 h and cooled to room temperature, and then 200 mL of an ammonium chloride saturated water solution was added to decompose the excess borohydride. The ethanol was removed under vacuum and the precipitated solid dissolved in a minimal amount of water. The resulting solution was extracted with ethyl acetate (5 ×

- (11) Lees, A. C.; Evrard, B.; Keyes, T. E.; Vos, J. G.; Kleverlaan, C. J.; Alebbi, M.; Bignozzi, C. A. *Eur. J. Inorg. Chem.* **1999**, 2309–2317.  
 (12) (a) Kelly, C. A.; Farzad, F.; Thompson, D. W.; Meyer, G. J. *Langmuir* **1999**, *15*, 731–737. (b) Kelly, C. A.; Farzad, F.; Thompson, D. W.; Stipkala, J. M.; Meyer, G. J. *Langmuir* **1999**, *15*, 7047–7054.  
 (13) (a) Penicaud, V.; Odobel, F.; Bujoli, B. *Tetrahedron Lett.* **1998**, *39*, 3689–3692. For other conditions for the preparation of bipyridine **7**, see: (b) Grätzel, M.; Kohle, O.; Nazeeruddin, M. K.; Péchy, P.; Royzinger, F. P.; Ruile, S.; Zakeeruddin, S. M. PCT Int. Appl. WO 95029, 924 (Cl. CO7F9/58) 9 Nov 1995, Appl94/IB88, 2 May 1994, 52 pp. (c) Athanassov, Y.; Rotzinger, F. P.; Péchy, P.; Grätzel, M. *J. Phys. Chem. B* **1997**, *101*, 2558–2563. (d) Montalti, M.; Wadhwa, S.; Kim, W. Y.; Kipp, R. A.; Schmehl, R. H. *Inorg. Chem.* **2000**, *39*, 76–84.  
 (14) Shklover, V.; Ovchinnikov, Y. E.; Braginsky, L. S.; Zakeeruddin, S. M.; Grätzel, M. *Chem. Mater.* **1998**, *10*, 2533–2541.

## Scheme 1. Preparation of Ligand 9



i)  $\text{K}_2\text{Cr}_2\text{O}_7/\text{H}_2\text{SO}_4$  (85%), ii)  $\text{EtOH}-\text{H}_2\text{SO}_4$  (90%), iii)  $\text{NaBH}_4-\text{EtOH}$  (81%),  
iv)  $\text{HBr}-\text{H}_2\text{SO}_4$  (85%), v)  $\text{P}(\text{OEt})_3$  (80%)

200 mL) and dried over sodium sulfate, and the solvent was removed under vacuum. The desired solid was obtained in 79% yield and was used without further purification.

$^1\text{H}$  NMR (300 MHz,  $\text{CD}_3\text{OD}$ ,  $\delta$ ): 4.75 (4H, s,  $\text{CH}_2$ ); 7.43 (2H, d,  $J = 5.5$  Hz, aryl H on  $\text{C}_5$  and  $\text{C}_5'$ ); 8.25 (2H, s, aryl H on  $\text{C}_3$  and  $\text{C}_3'$ ); 9.00 (2H, d,  $J = 5.5$  Hz, aryl H on  $\text{C}_6$  and  $\text{C}_6'$ ).

Elemental anal. Calcd for  $\text{C}_{12}\text{H}_{12}\text{N}_2\text{O}_2$ : C, 66.65; H, 5.59; N, 12.95. Found: C, 65.90; H, 5.70; N, 12.32.

**4,4'-Bis(bromomethyl)-2,2'-bipyridine (14).** The bipyridine **13** (0.90 g, 4.2 mmol) was dissolved in a mixture of 48% HBr (20 mL) and concentrated sulfuric acid (6.7 mL). The resulting solution was refluxed for 6 h and then allowed to cool to room temperature, and 40 mL of water was added. The pH was adjusted to neutral with NaOH solution and the resulting precipitate filtered, washed with water (pH = 7), and air-dried. The product was dissolved in chloroform (40 mL) and filtered. The solution was dried over magnesium sulfate and evaporated to dryness, yielding 1.2 g of **14** (85% yield) as a white powder.

$^1\text{H}$  NMR (300 MHz,  $\text{CDCl}_3$ ,  $\delta$ ): 4.50 (4H, s,  $\text{CH}_2$ ); 7.38 (2H, d,  $J = 5$  Hz, aryl H on  $\text{C}_5$  and  $\text{C}_5'$ ); 8.45 (2H, s, aryl H on  $\text{C}_3$  and  $\text{C}_3'$ ); 8.68 (2H, d,  $J = 5$  Hz, aryl H on  $\text{C}_6$  and  $\text{C}_6'$ ).

Elemental anal. Calcd for  $\text{C}_{12}\text{H}_{10}\text{N}_2\text{Br}_2$ : C, 42.14; H, 2.95; N, 8.19. Found: C, 42.03; H, 3.09; N, 8.38.

**4,4'-Bis(diethylmethylphosphonate)-2,2'-bipyridine (9).** A chloroform (10 mL) solution of **14** (1.5 g, 4.4 mmol) and 15 mL of triethyl phosphite was refluxed for 3 h under nitrogen. The excess phosphite was removed under high vacuum, and then the crude product was purified by column chromatography on silica gel (eluent ethyl acetate/methanol 80/20) yielding 1.6 g (80%) of **9** [4,4'-( $\text{CH}_2\text{PO}_3\text{Et}_2$ )<sub>2</sub>bpy].

$^1\text{H}$  NMR (300 MHz,  $\text{CDCl}_3$ ,  $\delta$ ): 1.29 (12H, t,  $J = 7$  Hz,  $\text{CH}_3$ ); 3.23 (4H, d,  $J = 22$  Hz,  $\text{CH}_2\text{P}$ ); 4.09 (8H, apparent quintet,  $J = 7$  Hz,  $\text{OCH}_2$ ); 7.35–7.38 (2H, m, aryl H on  $\text{C}_5$  and  $\text{C}_5'$ ); 8.34–8.37 (2H, m, aryl H on  $\text{C}_3$  and  $\text{C}_3'$ ); 8.62 (2H, d,  $J = 5$  Hz, aryl H on  $\text{C}_6$  and  $\text{C}_6'$ ).

$^{31}\text{P}$  NMR (81 MHz,  $\text{CDCl}_3$ ,  $\delta$ ): 25.37.

Elemental anal. Calcd for  $\text{C}_{20}\text{H}_{30}\text{N}_2\text{O}_6\text{P}_2$ : C, 52.63; H, 6.63; N, 6.14. Found: C, 52.83; H, 6.59; N, 6.01.

**[Ru(bpy)<sub>2</sub>(4,4'-( $\text{CH}_2\text{PO}_3\text{Et}_2$ )<sub>2</sub>bpy)]Cl<sub>2</sub>.** A solution of **9** (0.13 g, 0.29 mmol) and *cis*-[Ru(bpy)<sub>2</sub>Cl<sub>2</sub>] $\cdot 2\text{H}_2\text{O}^{10}$  (0.1 g, 0.18 mmol) in DMF (40 mL) was refluxed for 5 h under argon in the dark. The reaction mixture was evaporated to dryness and the crude product chromatographed on an LH20 column. Elution with methanol gave the orange desired product (first collected fraction), yielding 0.13 g (72%) of [Ru(bpy)<sub>2</sub>(4,4'-( $\text{CH}_2\text{PO}_3\text{Et}_2$ )<sub>2</sub>bpy)]Cl<sub>2</sub>.

$^1\text{H}$  NMR (300 MHz,  $\text{D}_2\text{O}$ ,  $\delta$ ): 0.96 (12H, t,  $J = 7$  Hz,  $\text{CH}_3$ ); 3.1 (4H, d,  $J = 21$  Hz,  $\text{CH}_2\text{P}$ ); 3.75 (8H, apparent quintet,  $J = 7$  Hz,  $\text{OCH}_2$ ); 7.12 (2H, m)  $\text{H}_5$ ,  $\text{H}_5'$ ; 7.20 (4H, m,  $\text{H}_{5a}$ ,  $\text{H}_{5a}'$ ); 7.52 (2H, m)  $\text{H}_6$ ,  $\text{H}_6'$ ; 7.72 (4H, m)  $\text{H}_{6a}$ ,  $\text{H}_{6a}'$ ; 7.87 (4H, m)  $\text{H}_{4a}$ ,  $\text{H}_{4a}'$ ; 8.27 (2H, m)  $\text{H}_3$ ,  $\text{H}_3'$ ; 8.36 (4H, d,  $J = 8$  Hz)  $\text{H}_{3a}$ ,  $\text{H}_{3a}'$ .

Elemental anal. Calcd for  $\text{RuC}_{40}\text{H}_{46}\text{N}_6\text{O}_6\text{P}_2\text{Cl}_2$ : C, 51.07; H, 4.93; N, 8.93. Found: C, 48.96; H, 5.01; N, 8.51.

**[Ru(bpy)<sub>2</sub>(4,4'-( $\text{CH}_2\text{PO}_3\text{H}_2$ )<sub>2</sub>bpy)]Cl<sub>2</sub> (4).** A solution of [Ru(bpy)<sub>2</sub>(4,4'-( $\text{CH}_2\text{PO}_3\text{Et}_2$ )<sub>2</sub>bpy)]Cl<sub>2</sub> (described above) (0.10 g, 0.013 mmol) in 20 mL of 18% HCl was refluxed for 8 h. The solvent was rotary evaporated and the resulting solid dried under vacuum to give 80 mg (90%) of the desired complex **4**.

$^1\text{H}$  NMR (300 MHz,  $\text{D}_2\text{O}$ ): 3.41 (4H, d,  $J = 21$  Hz,  $\text{CH}_2\text{P}$ ); 7.45 (2H, m)  $\text{H}_5$ ,  $\text{H}_5'$ ; 7.52 (4H, m)  $\text{H}_{5a}$ ,  $\text{H}_{5a}'$ ; 7.72 (2H, m)  $\text{H}_6$ ,  $\text{H}_6'$ ; 7.84 (4H, m)  $\text{H}_{6a}$ ,  $\text{H}_{6a}'$ ; 8.15 (4H, m)  $\text{H}_{4a}$ ,  $\text{H}_{4a}'$ ; 8.66 (2H, m)  $\text{H}_3$ ,  $\text{H}_3'$ ; 8.73 (4H, d,  $J = 8$  Hz)  $\text{H}_{3a}$ ,  $\text{H}_{3a}'$ .

Elemental anal. Calcd for  $\text{RuC}_{32}\text{H}_{30}\text{N}_6\text{O}_6\text{P}_2\text{Cl}_2$ : C, 46.39; H, 3.65; N, 10.14. Found: C, 46.78; H, 3.85; N, 10.13.

## Results and Discussion

**Synthesis.** Four different anchoring bipyridines have been synthesized for this study, Chart 1. They differ by the substitution positions of the phosphonic groups, i.e., 4,4' versus 5,5', and by the connection mode of the  $\text{PO}_3\text{H}_2$  group to the bipyridine core, i.e., presence or absence of a  $\text{CH}_2$  spacer. We had previously found that a direct link between the sensitizer and the semiconductor is not a strict requirement for high electron injection efficiency.<sup>6</sup> Therefore, complexes derived from bipyridines **8** or **9** may advantageously replace those derived from ligands **6** and **7** whose preparation is more complex. Utilization of a spacer group between the phosphonic acid and the bipyridine ligand can also open the door to designing sensitizers with light-harvesting antenna positioned a considerable distance away from the semiconductor surface. In addition, on the basis of geometrical considerations with idealized structures, it has been suggested that only one carboxylic acid group needs to attach to the surface for efficient energy conversion.<sup>14</sup> As a consequence, there may be no disadvantage to positioning the anchoring groups in the 5,5' position of the bipyridine ligand where simultaneous binding of both phosphonic acids to the same nanoparticle is geometrically unfavorable. Furthermore, the magnitude of the electronic communication with the semiconductor may also vary with the substitution position. It seems, therefore, of high importance to consider these issues in the rational development of sensitizers for efficient solar cells.

To probe the influence of substitutional variations, five ruthenium complexes **1**, **2**, **3**, **4**, and **5** have been prepared and studied. Ligands **6**<sup>13</sup> and **7**<sup>13</sup> have been prepared by palladium cross coupling reaction of diethyl phosphite with the corresponding dibromo bipyridine according to the Hirao procedure.<sup>15</sup> Ligands **8**<sup>16</sup> and **9** were obtained by Arbuzov reaction between triethyl phosphite and bis(bromomethyl)bipyridine. Since monohalogenation of the methyl group of 4,4'-dimethyl-2,2'-bipyridine with *N*-bromosuccinimide is difficult to achieve selectively, the preparation of this compound was best performed according to the five-step route illustrated in Scheme 1.

This procedure involves oxidation of the methyl groups to carboxylic acids with potassium dichromate. The subsequent esterification with ethanol, reduction of the ester to the alcohol with sodium borohydride, substitution with hydrobromic acid, and reaction with triethyl phosphite yields the desired bipyridine **9** in 56% overall yield. Preparation of the ruthenium complexes was achieved by reaction of *cis*-Ru(bpy)<sub>2</sub>Cl<sub>2</sub> with 1 equiv of the bisphosphonate bipyridine ligand according to standard

(15) Hirao, T.; Masunaga, T.; Ohshiro, Y.; Agawa, T. *Synthesis* **1981**, 56–59.

(16) Peng, Z.; Gharavi, A. R.; Yu, L. *J. Am. Chem. Soc.* **1997**, *119*, 4622–4632.

**Table 1.** Spectroscopic and Redox Properties of the Complexes

metal complex <sup>a</sup>	$\lambda_{\text{abs max}}$ (nm) <sup>b</sup> [ $\epsilon$ (M <sup>-1</sup> cm <sup>-1</sup> )]	$\lambda_{\text{em max}}$ (nm) <sup>c</sup>	$\tau$ (ns) <sup>c</sup>	$E_{1/2}^d$ (V) (Ru <sup>III/II</sup> )
[Ru(bpy) <sub>2</sub> (4,4'-(CH <sub>2</sub> PO <sub>3</sub> H <sub>2</sub> ) <sub>2</sub> bpy)]Cl <sub>2</sub> <b>4</b>	454 [13100]	632	890	1.26
[Ru(bpy) <sub>2</sub> (4,4'-(PO <sub>3</sub> H <sub>2</sub> ) <sub>2</sub> bpy)]Br <sub>2</sub> <b>1</b>	458 [9300]	650	740	1.36
[Ru(bpy) <sub>2</sub> (5,5'-(CH <sub>2</sub> PO <sub>3</sub> H <sub>2</sub> ) <sub>2</sub> bpy)]Br <sub>2</sub> <b>3</b>	452 [11100]	630	675	1.29
[Ru(bpy) <sub>2</sub> (5,5'-(PO <sub>3</sub> H <sub>2</sub> ) <sub>2</sub> bpy)]Br <sub>2</sub> <b>2</b>	458 [15700]	660	200	1.37
[Ru(bpy) <sub>2</sub> (4,4'-(CO <sub>2</sub> H) <sub>2</sub> bpy)](PF <sub>6</sub> ) <sub>2</sub> <b>5</b>	477 <sup>e</sup> [14000]	680 <sup>e</sup>	800 <sup>e</sup>	1.38

<sup>a</sup> The metal complexes used as sensitizers where bpy is 2,2'-bipyridine. The bold numbers represent the abbreviations for the complexes used throughout the text. <sup>b</sup> Absorption maximum,  $\pm 2$  nm, measured in methanol unless otherwise noted. The molar extinction coefficients at these wavelengths are given in brackets. <sup>c</sup> Emission maximum,  $\pm 4$  nm, and lifetime,  $\pm 5$  ns, measured in argon-saturated methanol solutions unless otherwise noted. <sup>d</sup> Half-wave potentials for the Ru<sup>III/II</sup> couple measured in CH<sub>3</sub>CN electrolyte containing 0.1 M HClO<sub>4</sub> versus an SCE reference electrode. <sup>e</sup> Measured in argon-saturated acetonitrile.

preparations.<sup>17</sup> The ethyl phosphonate ester was hydrolyzed during this reaction, and was retrieved partly in its monoester form at the end of the reaction following a procedure reported by other groups.<sup>7b,d</sup> It could be purified on silica gel before being fully hydrolyzed by refluxing in hydrobromic acid or by adding bromotrimethylsilane in dimethylformamide.

**Spectroscopic and Redox Properties.** Spectroscopic and photophysical properties of the complexes were studied in methanol. The absorption spectra of these complexes are typical of the ruthenium polypyridyl complexes with intense UV bands, assigned to ligand-centered  $\pi-\pi^*$  transitions, and broad bands in the visible region due to metal-to-ligand charge-transfer (MLCT) transitions. The data are summarized in Table 1.

Excitation into the MLCT manifold leads to room temperature photoluminescence in deoxygenated methanol solution. Time-resolved photoluminescence decays are satisfactorily fit to a first-order kinetic model, Table 1. The electron-withdrawing nature of phosphonic acid groups lowers the energy of the  $\pi^*$ -orbital of the bipyridine ligand and, hence, the energy level of the MLCT excited state. As a weak electronic donating group, CH<sub>2</sub>PO<sub>3</sub>H<sub>2</sub> does the opposite. The red shift of the emission for **1** and **2** with respect to [Ru(bpy)<sub>3</sub>]<sup>2+</sup> is consistent with localization of the excited electron on the phosphonated bipyridine ligand.<sup>18</sup> The magnitude of the perturbation depends on the extent of electronic communication between the phosphonic acid group and the pyridine fragment. The inductive effects observed spectroscopically are also manifest in the electrochemical properties, as discussed below.

Time-resolved absorption difference spectra of complexes **1–4** anchored to colloidal ZrO<sub>2</sub> thin films were recorded after pulsed 532.5 nm light excitation in 0.1 M LiClO<sub>4</sub> acetonitrile solutions at 25 °C, Figure 1. The absorption difference spectra of all complexes are qualitatively similar and assigned to the MLCT excited state with characteristic absorptions from the reduced ligand at  $\sim 380$  nm, a bleach of the MLCT charge-transfer band at  $\sim 450$  nm, and clean isosbestic points at  $\sim 400$  and  $\sim 510$  nm. These isosbestic points are important for interfacial electron transfer studies as they allow us to selectively monitor the electron-transfer products, as described further below.

The electrochemical properties of the sensitizers were explored by cyclic voltammetry. The measurements were performed in acetonitrile solutions acidified with perchloric acid to improve the solubility of the bromide salts of the complexes.

All complexes studied exhibited quasi-reversible waves assigned to the Ru<sup>III/II</sup> couple, Table 1. The increase of the metal-based Ru<sup>III/II</sup> reduction potential in complexes **1** and **2**, compared to complexes **3** and **4**, reflects less electron density on the substituted bipyridine ligand due to the electron-withdrawing phosphonic acid groups. Clearly, the  $-\text{CH}_2-$  spacer changes the nature of the electronic interaction between bipyridine ligand and the substituents. As a result, the Ru<sup>III/II</sup> reduction potential in complexes **1** and **2** is increased by  $\sim 100$  mV relative to complexes **3** and **4**.

**Surface Binding Experiments.** An important goal for the preparation of economically viable dye-sensitized photovoltaic cells is to develop a strong and stable sensitizer–semiconductor attachment. The semiconductor-bound sensitizers should withstand prolonged exposure to electrolyte solutions and the ambient. The adduct formation constants for the phosphonic acid groups on TiO<sub>2</sub> were estimated by measuring the adsorption isotherm of complexes **1** and **5** in methanol. In these experiments, five TiO<sub>2</sub> films were immersed in  $10^{-3}$ – $10^{-5}$  M methanol solutions of the complexes for 48 h at 20 °C. The concentrations of the bound sensitizers were determined spectroscopically, and adsorption isotherms were constructed. The surface binding was found to follow the Langmuir model, and adduct formation constants were abstracted from this analysis.<sup>6</sup> Adduct formation constants for complexes disubstituted in the 5,5' positions,  $K_3 = (5.2 \pm 0.6) \times 10^4 \text{ M}^{-1}$  and  $K_2 = (3.1 \pm 0.3) \times 10^4 \text{ M}^{-1}$ , are an order of magnitude lower than those for the 4,4'-disubstituted phosphonic acids, presumably because only one phosphonic acid group is able to bind to the semiconductor surface in the 5,5'-disubstituted geometry. For sensitizers with functional groups in the 4 and 4' positions, there is approximately a 1 order of magnitude increase in the adduct formation constant for phosphonic acid containing sensitizers than for carboxylic acids:  $K_4 = (4.9 \pm 0.8) \times 10^5 \text{ M}^{-1}$  and  $K_1 = (1.3 \pm 0.2) \times 10^5 \text{ M}^{-1}$  compared to  $K_5 = (2.2 \pm 0.1) \times 10^4 \text{ M}^{-1}$ . The lower binding constant for **5** indicates that the phosphonic acid groups provide stronger and more stable linkages to TiO<sub>2</sub> than do carboxylic acid groups under these conditions. Surface desorption experiments in pH 5.7 aqueous solutions showed that 90% of complex **5** desorbed from TiO<sub>2</sub> after 1 h, compared to only 30–35% desorption for the phosphonated complexes **1–4**. Chemisorption of phosphonic

- (17) (a) Belser, P.; von Zelewsky, A.; Frank, M.; Vögtle, F.; De Cola, L.; Barigelletti, F.; Balzani, V. *J. Am. Chem. Soc.* **1993**, *115*, 4076–4086. (b) De Cola, L.; Balzani, V.; Barigelletti, F.; Flamigni, L.; Belser, P.; von Zelewsky, A.; Franck, M.; Vögtle, F. *Inorg. Chem.* **1993**, *32*, 5228–5238.
- (18) Juris, A.; Balzani, V.; Barigelletti, F.; Campagna, S.; Belser, P.; Von Zelewsky, A. *Coord. Chem. Rev.* **1988**, *84*, 85–277.

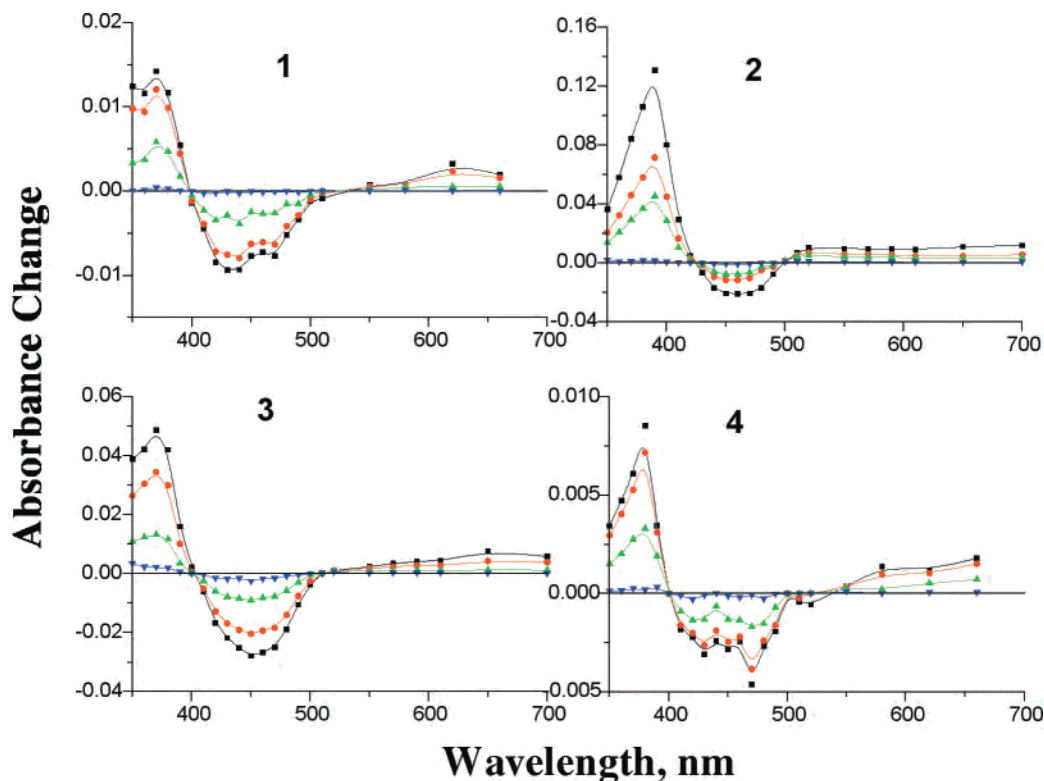


**Figure 1.** Time-resolved absorption difference spectra observed after 532.5 nm pulsed laser light excitation ( $\sim 10 \text{ mJ cm}^{-2}$ , 8 ns fwhm) of the Ru(II) compounds bound to nanocrystalline  $\text{ZrO}_2$  films in 0.1 M  $\text{LiClO}_4$  argon-purged acetonitrile electrolyte at 25 °C: (1) **1**  $\text{Ru}(\text{bpy})_2(4,4'-(\text{PO}_3\text{H}_2)_2\text{bpy})^{2+}$ , (2) **2**  $\text{Ru}(\text{bpy})_2(5,5'-(\text{PO}_3\text{H}_2)_2\text{bpy})^{2+}$ , (3) **3**  $\text{Ru}(\text{bpy})_2(5,5'-(\text{CH}_2\text{PO}_3\text{H}_2)_2\text{bpy})^{2+}$ , and (4) **4**  $\text{Ru}(\text{bpy})_2(4,4'-(\text{CH}_2\text{PO}_3\text{H}_2)_2\text{bpy})^{2+}$ . The data were recorded at 0 ns (squares), 50 ns (circles), 500 ns (triangles), and 2  $\mu\text{s}$  (upside-down triangles) delays after the laser pulse.

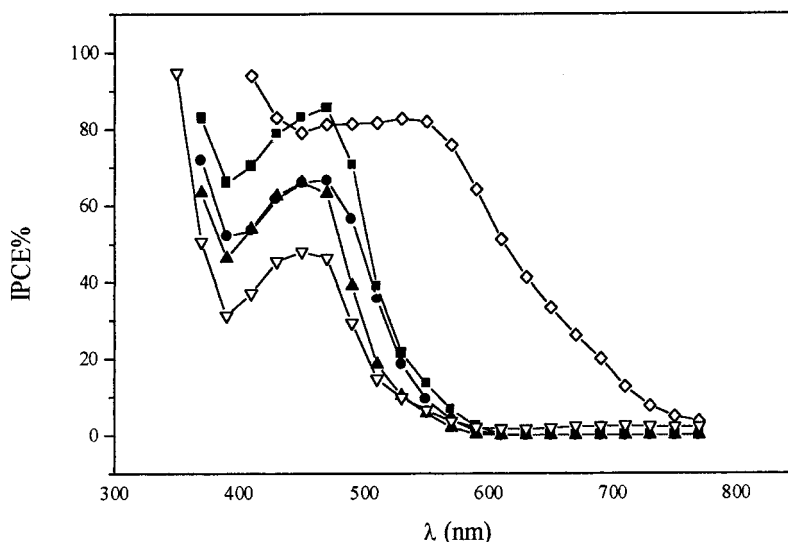


**Figure 2.** Incident photon-to-current efficiency conversion, IPCE, vs excitation wavelength for **1** (squares)  $[\text{Ru}(\text{bpy})_2(4,4'-(\text{PO}_3\text{H}_2)_2\text{bpy})]\text{Br}_2$  (1.2), **2** (circles)  $[\text{Ru}(\text{bpy})_2(5,5'-(\text{PO}_3\text{H}_2)_2\text{bpy})]\text{Br}_2$  (0.9), **3** (triangles)  $[\text{Ru}(\text{bpy})_2(5,5'-(\text{CH}_2\text{PO}_3\text{H}_2)_2\text{bpy})]\text{Br}_2$  (0.8), **4** (upside-down triangles)  $[\text{Ru}(\text{bpy})_2(4,4'-(\text{CH}_2\text{PO}_3\text{H}_2)_2\text{bpy})]\text{Cl}_2$  (0.8), and **5** (diamonds)  $\text{Ru}(4,4'-(\text{CO}_2\text{H})_2\text{bpy})_2(\text{NCS})_2$  (1.0). Values in parentheses represent the maximum absorbance, in absorbance units, of the investigated photoanode. The IPCE measurements were made in 0.5 M  $\text{LiI}/0.05 \text{ M I}_2$  in acetonitrile at room temperature.

acids may yield a strong covalent bond similar to those found in titanium phosphonates.<sup>19</sup> Phosphonic acid is therefore an attractive binding group to engineer photoactive semiconductor electrodes for molecular devices.

**Photoelectrochemical Properties.** The photoelectrochemical performances of the sensitizers were studied on transparent  $\text{TiO}_2$  nanocrystalline electrodes in regenerative solar cells with a 0.5

M  $\text{LiI}/0.05 \text{ M I}_2$  acetonitrile electrolyte.<sup>1</sup> The photoaction spectra of **1–5** are shown in Figure 2, where the incident photon-to-current efficiencies (IPCE) are plotted as a function of the excitation wavelength. The photoaction spectrum of  $\text{Ru}(4,4'-(\text{CO}_2\text{H})_2\text{bpy})_2(\text{NCS})_2$ , which is one of the most efficient sensitizers known under solar irradiance conditions,<sup>1b</sup> is also shown in Figure 2 for comparison purposes. At individual wavelengths of light, complex **1** converts light to electricity as efficiently as  $\text{Ru}(4,4'-(\text{CO}_2\text{H})_2\text{bpy})_2(\text{NCS})_2$ . However, **1** does not harvest light in the red region and would therefore perform

(19) Olivera-Pastor, P.; Maireles-Torres, P.; Rodríguez-Castellón, E.; Jiménez-López, A. *Chem. Mater.* **1996**, *8*, 1758–1769.

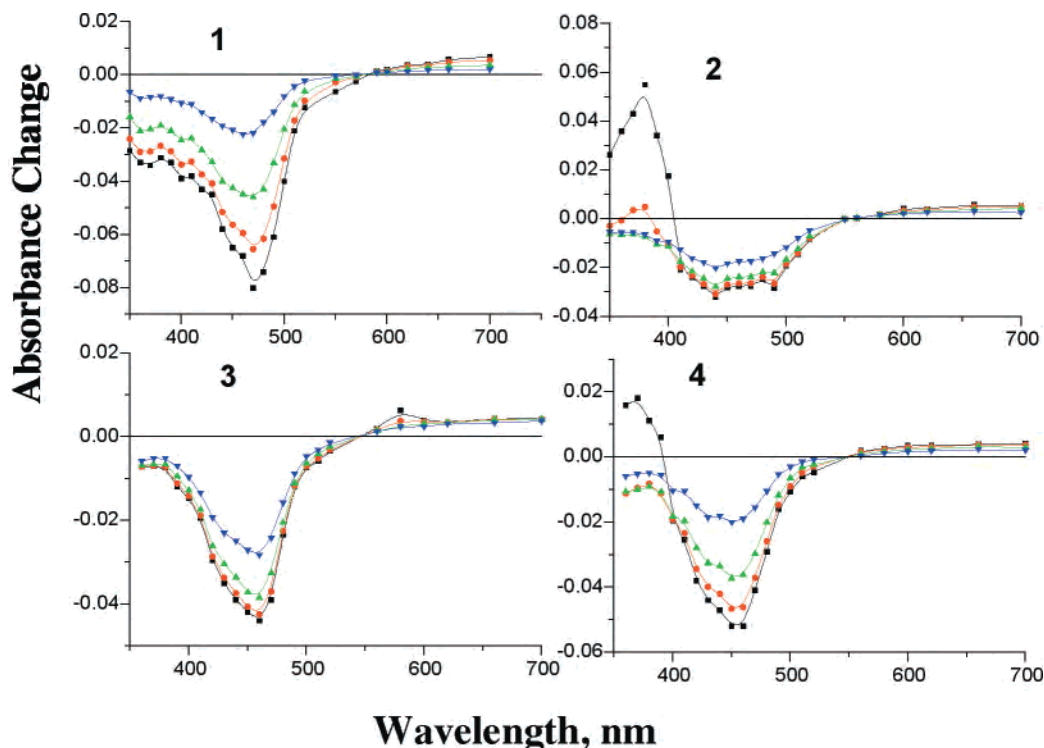


**Figure 3.** Time-resolved absorption difference spectra observed after 532.5 nm pulsed laser light excitation ( $\sim 10 \text{ mJ cm}^{-2}$ , 8 ns fwhm) of the Ru(II) compounds bound to nanocrystalline TiO<sub>2</sub> films in 0.1 M LiClO<sub>4</sub> argon-purged acetonitrile electrolyte at 25 °C: (1) **1** Ru(bpy)<sub>2</sub>(4,4'-(PO<sub>3</sub>H<sub>2</sub>)<sub>2</sub>bpy)<sup>2+</sup>, (2) **2** Ru(bpy)<sub>2</sub>(5,5'-(PO<sub>3</sub>H<sub>2</sub>)<sub>2</sub>bpy)<sup>2+</sup>, (3) **3** Ru(bpy)<sub>2</sub>(5,5'-(CH<sub>2</sub>PO<sub>3</sub>H<sub>2</sub>)<sub>2</sub>bpy)<sup>2+</sup>, and (4) **4** Ru(bpy)<sub>2</sub>(4,4'-(CH<sub>2</sub>PO<sub>3</sub>H<sub>2</sub>)<sub>2</sub>bpy)<sup>2+</sup>. The data were recorded at 0 ns (squares), 50 ns (circles), 500 ns (triangles), and 2  $\mu\text{s}$  (upside-down triangles) delays after the laser pulse.

less efficiently under the sun. In all cases, the photoaction and absorbance spectra are the same, within reasonable experimental error, indicating that light absorption by the sensitizer occurs prior to electron injection into the semiconductor.<sup>11</sup>

Complex **1** gives the highest IPCE, complexes **2** and **3** are within experimental error the same, while complex **4** is far less efficient. When the phosphonate groups are directly attached to the bipyridine ring, changing their positions from 4,4' to 5,5' results in a minor decrease in the IPCE. The introduction of a methylene spacer has a dramatic effect for the 4,4'-disubstituted sensitizers, but is not significant for the 5,5'-disubstituted sensitizers.

To rationalize the trends in photocurrent efficiency observed for the different sensitizers, consider that the IPCE is the product of three terms:

$$\text{IPCE} = (\text{LHE})\phi\eta$$

where LHE is the light-harvesting efficiency,  $\phi$  is the quantum yield for electron injection from the excited sensitizer to the semiconductor, and  $\eta$  is the efficiency of collecting electrons in the external circuit. The LHE is the fraction of light absorbed by the material and was controlled to be nearly the same for all the Ru<sup>II</sup> complexes. If corrections are made for the LHE, we find that the absorbed photon-to-current efficiency is nearly the same for **1–3** but is significantly lower for **4**. The  $\eta$  term has been related to the kinetics for reduction of the oxidized sensitizer and electron donor.<sup>11</sup> Since all investigated complexes have very positive Ru<sup>III/II</sup> reduction potentials, regeneration by iodide will be rapid and  $\eta$  is expected to be the same for all the sensitizers studied.<sup>20,21</sup> Therefore, by process of elimination, the term most likely to account for the lower IPCE measured for **4** is the interfacial electron injection quantum yield,  $\phi$ .

**Interfacial Electron Injection.** Nanosecond absorption spectroscopy was used to determine the rates and yields for

interfacial electron transfer. Absorption difference spectra of complexes **1–4** bound to TiO<sub>2</sub> were recorded after pulsed 532.5 nm light excitation in 0.1 M LiClO<sub>4</sub> acetonitrile solution at 25 °C, Figure 3. The presence of MLCT excited states at short delay times is clearly evident in the spectra of **4**, indicating that the quantum yield for electron injection is less than unity. The appearance of excited states for this and other sensitizers can complicate analysis of interfacial electron-transfer kinetics and yields by transient absorption spectroscopy. To circumvent this complication, transient absorption measurements were made at wavelengths where the ground and excited states absorb light equally, i.e., isosbestic points. The isosbestic points were determined on colloidal ZrO<sub>2</sub> films, Figure 1, and were assumed to be the same on TiO<sub>2</sub>. In support of this assumption, we found that isosbestic points do not vary significantly with environment and those measured on ZrO<sub>2</sub> films were within  $\pm 5$  nm of those measured in fluid acetonitrile solution. The isosbestic point at  $\sim 400$  nm observed for all the sensitizers was chosen because the oxidized sensitizers absorb very weakly at this wavelength, relative to the ground state, resulting in a strong  $\Delta A$  bleach under conditions of electron injection. The isosbestic point near 510 nm was also more difficult to monitor due to increased scatter from the 532.5 nm excitation source. In summary, by monitoring

(20) (a) Tachibana, Y.; Moser, J. E.; Grätzel, M.; Klug, D. R.; Durrant, J. *J. Phys. Chem.* **1996**, *100*, 20056. (b) Hannappel, T.; Burfeindt, B.; Storck, W.; Willig, F. *J. Phys. Chem. B* **1997**, *101*, 6799. (c) Heimer, T. A.; Heilweil, E. J. *J. Phys. Chem. B* **1997**, *101*, 10990. (d) Ellingson, R. J.; Asbury, J. B.; Ferrere, S.; Ghosh, H. N.; Sprague, J. R.; Lian, T.; Nozik, A. J. *J. Phys. Chem. B* **1998**, *102*, 6455.

(21) The 100 mV difference in the Ru(II)/III reduction potentials between phosphonates with and without the CH<sub>2</sub> spacer could also affect the IPCE through changes in  $\eta$ . However, we expect this to be of minor importance since other sensitizers with much more negative Ru(III)/II potentials efficiently oxidize iodide after electron injection; see ref 1 for example. Therefore, we expect rapid and quantitative sensitizer regeneration by iodide for all compounds studied.

absorption changes at the ground–excited state isosbestic point near 400 nm, the interfacial electron-transfer products can be cleanly observed with high signal-to-noise ratios without unwanted contributions from excited states.

The formation of the interfacial charge-separated pair,  $[\text{TiO}_2(\text{e}^-)|\text{Ru}^{\text{III}}]$ , was instrument response limited in all cases, indicating that  $k_{\text{inj}} > 10^8 \text{ s}^{-1}$ . Charge recombination of the injected electron and the oxidized sensitizer requires milliseconds for completion. This lower limit for the rate constant would suggest injection quantum yields near unity if injection were occurring in competition with radiative and nonradiative decay from the emissive excited state. In fact the injection yields are not all unity (see below), and this indicates that injection occurs from vibrationally “hot” excited states and in competition with vibrational relaxation. “Hot” injection has previously been proposed for **5** and is consistent with many ultrafast, femto-second spectroscopic studies.<sup>12b,20</sup> The observed transients are typical for charge recombination and were not quantified in further detail here.<sup>6,7</sup> Ground-state absorption spectra recorded before and after time-resolved absorption studies gave no evidence for surface desorption or sensitizer decomposition.

Comparative actinometry measurements were utilized to quantify the injection quantum yields,  $\phi$ , of compounds **1–4**: **1**,  $\phi = 1.0 \pm 0.1$ ; **2**,  $\phi = 0.6 \pm 0.1$ ; **3**,  $\phi = 0.6 \pm 0.1$ ; and **4**  $\phi = 0.5 \pm 0.1$ . The trend in  $\phi$  follows the trend in IPCE and suggests that the photocurrent efficiency is dictated by the injection quantum yield. We emphasize that a direct correlation between the injection yields and IPCE measurements is not expected since the measurements are performed under different experimental conditions. An important difference is that the IPCE measurements are conducted in the presence of a redox active electrolyte,  $\text{I}^-/\text{I}_3^-$ , where the injection yields are not.

The variation in injection efficiency can be rationalized by considering inductive substituent effects on the  $\pi^*$  levels of the bipyridine ligand and the orientation of the excited state with respect to the semiconductor surface. For complex **1**, the MLCT excited state is localized on a surface-bound ligand and quantitative interfacial electron injection is observed. For **4**, the weak electron-donating nature of  $-\text{CH}_2\text{PO}_3\text{H}_2$  increased the  $\pi^*$  level of surface-bound ligand, and the MLCT excited state is most probably localized on the unsubstituted bipyridine ligands,

which are further from the  $\text{TiO}_2$  surface thereby decreasing the injection yield. We tentatively attribute the very comparable injection yields and photocurrent efficiencies of **2** and **3** to a surface-sensitizer orientation that allows both the substituted and unsubstituted bpy ligands' close approach to the semiconductor surface. Three-dimensional models show that, for **2** and **3**, only one of the phosphonic acid groups can bind to the semiconductor surface at one time. This orientation parks an unsubstituted bpy very close to the semiconductor where it can inject efficiently. While these explanations are consistent with observation, clearly more studies are needed to definitively define surface-semiconductor geometries and to fully rationalize the trends in photocurrent efficiency and injection quantum yield.

## Conclusions

A series of ruthenium bipyridyl complexes, represented by  $\text{Ru}(\text{bpy})_2(\text{bpy}')^{2+}$ , where  $\text{bpy}'$  is a bipyridine ligand substituted with phosphonic acid groups, were prepared and utilized for interfacial electron-transfer studies and light-to-electrical energy conversion. The highest photocurrent efficiency was observed for  $\text{Ru}(\text{bpy})_2(4,4'-(\text{PO}_3\text{H}_2)_2\text{-bpy})^{2+}$ , **1**, which converts light to electricity quantitatively at individual wavelengths of light. Introducing a methylene spacer between the phosphonate and the bipyridine ligand decreases the photocurrent efficiency and the electron injection quantum yield significantly. One important advantage of the phosphonic acid anchoring groups, compared to carboxylic acid groups, is the enhanced stability of the resulting linkage to the  $\text{TiO}_2$  surface.

**Acknowledgment.** This work was supported in part by a Commission-funded project called “High Integrated PV/Thermal Structural Components” under the JOULE-3 program (Contract JOR3-CT98-7040). We also thank CNRS for financial support and Daniel Maume (LDH in Ecole Vétérinaire in Nantes) for mass spectrometry measurements. The Division of Chemical Sciences, Office of Basic Energy Sciences, Office of Energy Research, U.S. Department of Energy, is gratefully acknowledged for research support for G.J.M. and P.Q.

IC010192E